

## Simulation of Magnet Thickness and Angle of Attack on Magnetic Force for Magnetic Turbine Design

Eka Pratama\*, Wirawan Wirawan

Mechanical Engineering, State Polytechnic of Malang, Jl. Soekarno Hatta 9, Malang, 65141, Indonesia  
\*Corresponding author: eka.pratama65100@gmail.com

### Article history:

Received: 15 January 2025 / Received in revised form: 23 March 2025 / Accepted: 11 April 2025  
Available online 17 July 2025

### ABSTRACT

Electric motors play a vital role across various industries. As their electricity demand grows, improving efficiency has become a priority. One area of innovation involves the use of magnetic strips for improving performance. This study aims to determine the magnet thickness and the angle of attack position in producing the strongest repulsive force in the magnetic turbine. The study used a simulation using SOLIDWORKS and EMS software, applying neodymium N52 magnets with varying sizes and angles of attack. The results indicate that the most efficient magnetic turbine configuration utilizes rotor and stator magnets with dimensions of  $\text{Ø}10 \times 20$  mm and an angle of attack of  $44^\circ$ . Magnet thickness influences the magnetic force: Thicker magnets generate stronger repulsive forces due to higher stored magnetic energy, whereas thinner magnets result in weaker forces due to reduced magnetization volume. The simulation of two opposing magnets confirmed that the configuration of  $\text{Ø}10 \times 20$  mm at a  $44^\circ$  angle of attack produced the highest magnetic flux density of  $2.277 \times 10^{-1}$  Tesla. Furthermore, the  $44^\circ$  angle between rotor and stator yielded a more stable magnetic flux distribution, effectively minimizing cogging torque, that a common cause of undesirable fluctuations in rotor motion. This angle can be recommended for achieving smoother and more efficient turbine operation.

Copyright © 2025. Journal of Mechanical Engineering Science and Technology.

Keywords: *Angle of attack, magnetic force, permanent magnet, rotor, stator.*

## I. Introduction

Electric motors use about 46% of the electricity produced globally, according to data on electricity usage worldwide [1]. This percentage is much larger than that of lighting applications. With 64% of industrial sector total energy consumption attributed to electric motor power usage, electric motors are clearly important in modern industrial activities [2]. This great dependence on electric machinery makes constant research and development necessary to raise the efficiency of electrical systems. One important trend is the general acceptance of permanent magnet electric motors. The Permanent Magnet Synchronous Motor (PMSM) is especially appealing since it might be more efficient, which would save energy and reduce heat production when the motor is fully loaded. PMSM motors can be up to 96.2% efficient when they are fully loaded, while induction motors can only be 93.6% efficient [3],[4]. This higher efficiency not only uses less energy, but it also helps keep energy sources going by relying less on fossil fuels [5].

The development of permanent magnet technology in electric motors has progressed rapidly, especially with the use of neodymium magnets ( $\text{Nd}_2\text{Fe}_{14}\text{B}$ ). Neodymium magnets have superior magnetic properties compared to conventional magnets such as alnico and ferrite. Neodymium magnets have a tetragonal crystal structure that produces uniaxial



magnetocrystalline anisotropy with a value of up to 7 T, which increases coercivity and resistance to demagnetization [6], [7]. In addition, neodymium magnets ( $\text{Nd}_2\text{Fe}_{14}\text{B}$ ) have a fairly high magnetic field strength ranging from 1.3 T to 1.6 T, and in magnets of this type, they can store quite a lot of energy, namely  $512 \text{ kJ/m}^3$  [8], [9]. Several studies have reported that the parameters of magnets, including magnet thickness and angle of attack, can influence the efficiency of an electric motor. The thickness of the magnet affects the strength of the magnetic field and the distribution of magnetic flux in the gap between the rotor and stator [10], and the angle of attack determines how the magnetic field interacts with the rotor. However, there are several obstacles such as unwanted magnetic resistance, unstable rotation, and less than maximum torque. This problem causes uneven flux distribution, so that the energy conversion efficiency value that occurs is automatically not optimal [11]. This study was carried out using simulation to determine the effect of magnetic field thickness and angle of attack in the rotor and stator design development process on magnetic turbines. So, the objective of this study is to improve the efficiency of the magnetic motor performance system and overcome the problem of energy loss caused by unexpected magnetic interactions.

## II. Material and Methods

### 1. Study Approach

The study approach involved a simulation process using SOLIDWORKS 2018 and the Electro-Magnetic Simulation Module (EMS) with variation of the magnet dimensions and the position of the angle of attack. To ensure consistency in each data collection, researchers control the main design parameters. The obtained data were analyzed using static data processing to validate the effects that occur on each variable tested to obtain the best parameters in this study.

### 2. Experimental Design

The flow of this research begins with a literature study to obtain information related to previous research (Figure 1). This can be a reference for determining variables in research and for finding phenomena that have been studied by previous researchers. Subsequently, the experimental design is constructed to conduct a systematic examination of variations in the size of the magnet and the angle of attack, while maintaining the same critical parameters, including the air gap and the configuration of the magnets. Various magnet configurations are tested under controlled settings using the SOLIDWORKS EMS module for simulation and data collection. Magnetic force intensity (N), magnetic field strength (A/m), and magnetic flux density are the main outputs. Data analysis examines how design elements affect magnetic interactions to optimize magnetic turbine efficiency. Interpreting simulation data, drawing conclusions, and suggesting practical implementation is the final phase.

This study's independent variables are the thickness of the magnets and the angle at which the rotor and stator hit each other. The magnetic force, namely the strength of the magnetic field and the density of the magnetic flux, is the dependent variable. These let us understand how the magnetic force is spread out in the simulation. Figure 2 shows the controlled variables, which include the type of magnet, the distance between the rotor and stator (air gap), the position of the magnet, the materials used for the rotor and stator, the spacing between aligned magnets, and the simulation parameters in SolidWorks 2018 with EMS.

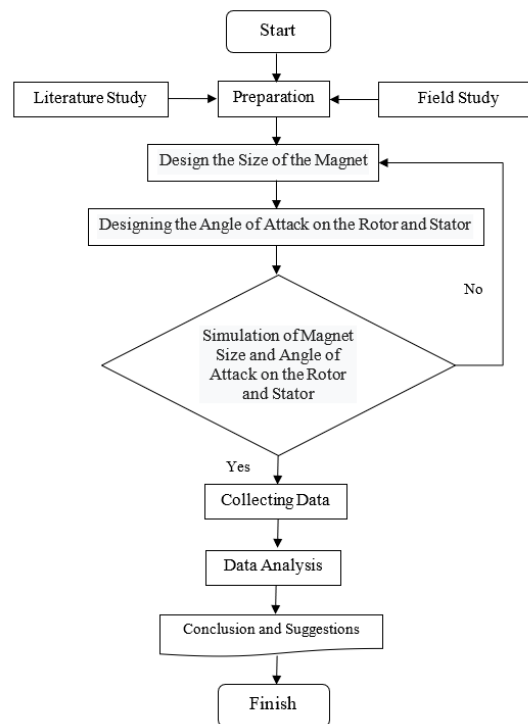


Fig. 1. Research flow chart

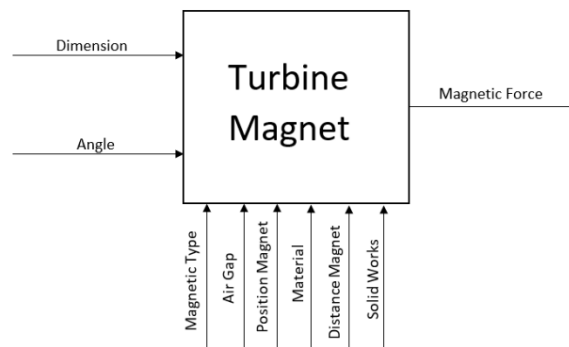


Fig. 2. Research variables

### 3. Experimental Parameters

#### *Magnet Size Variations*

To evaluate the effect of magnet size on repulsive force, this study tests four neodymium N52 magnet dimensions:  $\text{Ø } 10 \times 5 \text{ mm}$ ,  $\text{Ø } 10 \times 10 \text{ mm}$ ,  $\text{Ø } 10 \times 15 \text{ mm}$ , and  $\text{Ø } 10 \times 20 \text{ mm}$ . These sizes were chosen because they might change how magnetic force is spread out. The study looks at how variations in surface area exposure affect the creation of repulsion force by changing the thickness while keeping the diameter the same.

#### *Angle of Attack Variations*

In previous studies, it has been found that there is an influence of angle in determining the effectiveness of the repulsion force. The 3 angles found in previous studies are  $42^\circ$ ,  $44^\circ$ , and  $55^\circ$ . In addition, in this study, to ensure consistent positioning in data collection, the Air gap between the rotor and stator is set at 5 mm, while the magnet spacing remains at  $12^\circ$  and

the distance between the center points of the magnets on the rotor and stator is maintained at 90 mm, allowing for controlled comparisons across configurations.

### Material Selection

The rotor and stator are processed using 3D printing; this process can produce precise products using polyethylene material. The use of polyethylene is chosen because of its low shrinkage properties so that it can maintain the desired dimensions. In addition, polyethylene is also an insulator for electricity. This can prevent unwanted magnetic interference.

### 4. Simulation and Data Collection

Specifically, this study focuses on the value of the magnetic distribution by controlling the value of the magnetic field strength (A/m) and flux density (T). Concentration on the magnetic distribution value aims to determine the stable magnetic motor system, in order to produce efficient magnetic motor performance. The data collection process is carried out using a simulation method assisted by the SOLIDWORKS application and the EMS module. Furthermore, the simulation data results are analyzed to determine the best variables, namely, variables that produce the most efficient magnetic motor performance.

### 5. Interpretation of Simulation Results

Figures 3 visualize the magnetic field intensity with an angle between the rotor and stator of  $44^\circ$ . There are differences in the direction of the magnetic field intensity. In Figure 3A, the distribution of the magnetic field intensity is more attractive than repulsive. While in Figure 3B the distribution of the magnetic field intensity is more repulsive. In contrast, Figure 3B shows two magnets positioned directly opposite each other, revealing a concentrated repulsive force at the magnet's surface. This aligns with theoretical expectations, as identical poles generate strong repulsion when facing each other directly. The force distribution is visualized using color-coded intensity maps, allowing for a comparative analysis of repulsion efficiency across different configurations.

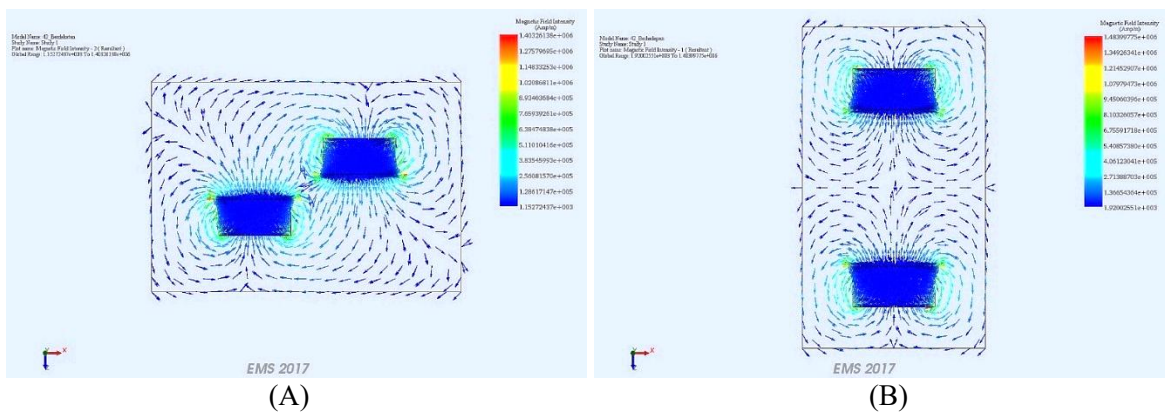


Fig. 3. Position of two adjacent magnets (A); Two magnets facing each other (B)

Figures 4 focus on rotor-stator interactions, where multiple magnets are arranged on the stator while a single magnet is positioned on the rotor. Figure 4A illustrates a direct alignment between rotor and stator magnets, revealing the intensity of repulsion at varying angles of attack. Meanwhile, Figure 4B examines an offset configuration, highlighting how changes in magnet positioning influence repulsive force magnitude. These results help determine the most effective design parameters for achieving optimal turbine motion.

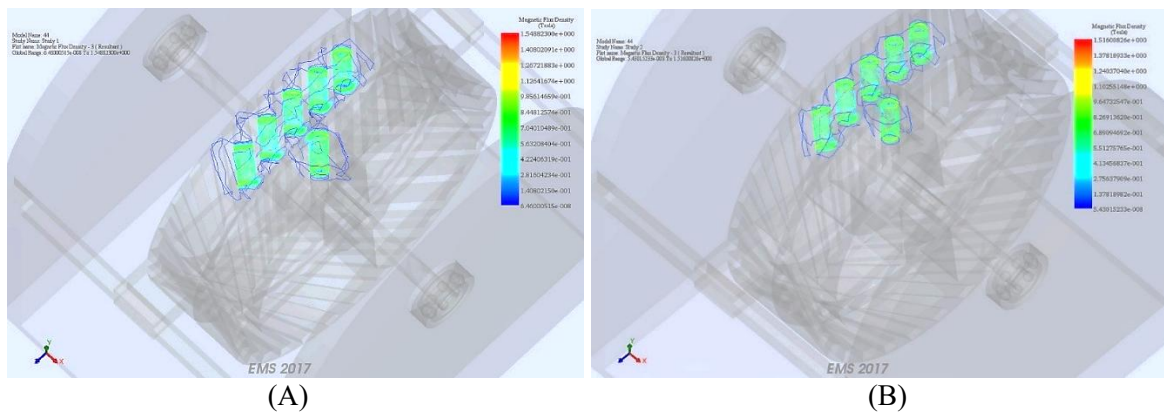


Fig. 4. Rotor and stator magnets: facing each other (A); Adjacent magnets (B)

### III. Results and Discussions

The simulation results presented in Tables 1–6 indicate that the intensity of the magnetic field and the magnetic flux density vary depending on the thickness of the magnets, the angle of attack, and their relative positioning. The variations observed in the results can be attributed to the interaction between magnetic fields, which is influenced by both the physical dimensions of the magnets and their spatial arrangement.

#### 1. Influence of Magnet Thickness and Angle of Attack on Field Intensity and Flux Density

Results of the thickness variation and adjacent magnet attack angle are depicted in Figure 5. Tables 1 and 2 show that the magnet with a size of  $\text{Ø } 10 \times 20 \text{ mm}$  at a  $42^\circ$  angle of attack produces the highest magnetic field intensity ( $1.884 \times 10^5 \text{ A/m}$ ) and magnetic flux density ( $2.046 \times 10^{-1} \text{ T}$ ) when two magnets are facing each other. This is because thicker magnets store more magnetic energy, leading to a stronger magnetic field [13]. On the other hand, the  $\text{Ø } 10 \times 5 \text{ mm}$  magnet at a  $44^\circ$  angle of attack produces the lowest magnetic field intensity and flux density, indicating that thinner magnets generate weaker magnetic fields due to their lower magnetization volume [14].

**Table 1.** Magnetic field intensity on the thickness and angle of attack of facing magnets

Magnet size	Magnetic field intensity (A/m) at angle of attack		
	$42^\circ$	$44^\circ$	$55^\circ$
$\text{Ø } 10 \times 5 \text{ mm}$	$1.366 \times 10^5$	$1.109 \times 10^5$	$1.258 \times 10^5$
$\text{Ø } 10 \times 10 \text{ mm}$	$1.202 \times 10^5$	$1.327 \times 10^5$	$1.296 \times 10^5$
$\text{Ø } 10 \times 15 \text{ mm}$	$1.836 \times 10^5$	$1.529 \times 10^5$	$1.545 \times 10^5$
$\text{Ø } 10 \times 20 \text{ mm}$	$1.884 \times 10^5$	$1.759 \times 10^5$	$1.780 \times 10^5$

**Table 2.** Magnetic flux density on the thickness and angle of attack of facing magnets

Magnet size	Magnetic flux density (T) at angle of attack		
	$42^\circ$	$44^\circ$	$55^\circ$
$\text{Ø } 10 \times 5 \text{ mm}$	$1.726 \times 10^{-1}$	$1.404 \times 10^{-1}$	$1.591 \times 10^{-1}$
$\text{Ø } 10 \times 10 \text{ mm}$	$1.542 \times 10^{-1}$	$1.702 \times 10^{-1}$	$1.637 \times 10^{-1}$
$\text{Ø } 10 \times 15 \text{ mm}$	$2.357 \times 10^{-1}$	$1.965 \times 10^{-1}$	$1.986 \times 10^{-1}$
$\text{Ø } 10 \times 20 \text{ mm}$	$2.046 \times 10^{-1}$	$2.277 \times 10^{-1}$	$2.237 \times 10^{-1}$

A similar trend is observed in the adjacent magnet configuration (Tables 3 and 4). However, in this case, the magnet with  $\text{Ø } 10 \times 20 \text{ mm}$  at  $42^\circ$  still exhibits the highest values for both magnetic field intensity ( $1.777 \times 10^5 \text{ A/m}$ ) and magnetic flux density ( $2.235 \times 10^{-1} \text{ T}$ ). This suggests that even when magnets are positioned adjacently rather than facing each other, thickness remains a dominant factor in determining the magnetic field strength [15].

**Table 3.** Magnetic field intensity on the thickness and angle of attack of adjacent magnets

Magnet size	Magnetic field intensity (A/m) at angle of attack		
	$42^\circ$	$44^\circ$	$55^\circ$
$\text{Ø } 10 \times 5 \text{ mm}$	$1.286 \times 10^5$	$1.371 \times 10^5$	$1.569 \times 10^5$
$\text{Ø } 10 \times 10 \text{ mm}$	$1.483 \times 10^5$	$1.514 \times 10^5$	$1.719 \times 10^5$
$\text{Ø } 10 \times 15 \text{ mm}$	$1.686 \times 10^5$	$1.596 \times 10^5$	$1.585 \times 10^5$
$\text{Ø } 10 \times 20 \text{ mm}$	$1.777 \times 10^5$	$1.741 \times 10^5$	$1.732 \times 10^5$

**Table 4.** Magnetic flux density on the thickness and angle of attack of adjacent magnets

Magnet size	Magnetic flux density (T) at angle of attack		
	$42^\circ$	$44^\circ$	$55^\circ$
$\text{Ø } 10 \times 5 \text{ mm}$	$1.616 \times 10^{-1}$	$1.723 \times 10^{-1}$	$1.984 \times 10^{-1}$
$\text{Ø } 10 \times 10 \text{ mm}$	$1.879 \times 10^{-1}$	$1.902 \times 10^{-1}$	$2.181 \times 10^{-1}$
$\text{Ø } 10 \times 15 \text{ mm}$	$2.173 \times 10^{-1}$	$2.056 \times 10^{-1}$	$2.048 \times 10^{-1}$
$\text{Ø } 10 \times 20 \text{ mm}$	$2.235 \times 10^{-1}$	$2.212 \times 10^{-1}$	$2.234 \times 10^{-1}$

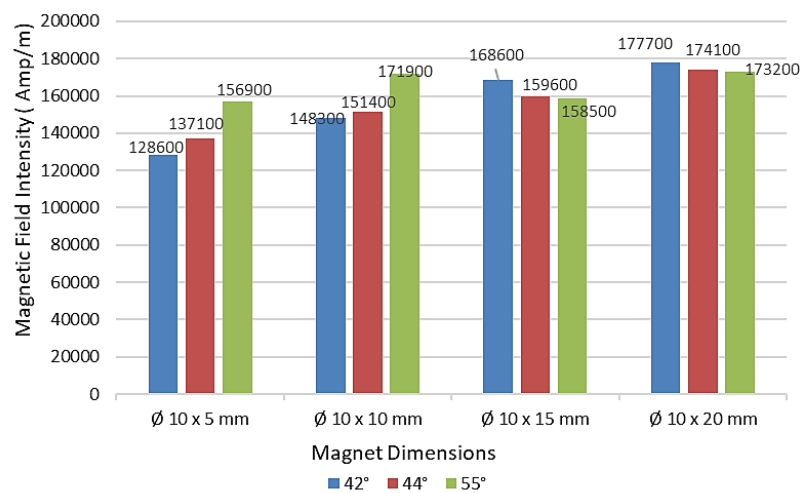


Fig. 5. Results of the thickness variation and adjacent magnet attack angle

## 2. Comparison Between Facing and Adjacent Magnets

The results show that the magnetic field intensity and flux density are higher when the magnets are facing each other compared to when they are adjacent. This can be explained when two magnets face each other; they exert direct repulsive or attractive forces, resulting in a stronger concentration of the magnetic field between them [16]. In contrast, adjacent magnets interact through side forces, leading to a more diffused field distribution and a relatively lower intensity [17].

### 3. Influence of Magnet Angle and Position in a Magnetic Turbine Arrangement

Tables 5 and 6 present data on the influence of angle of attack and rotor rotation on magnetic field intensity and flux density in a magnetic turbine setup. The results of the variation of magnet angle and position are presented in Figure 6. The results show that when magnets are aligned at a  $42^\circ$  angle of attack and the rotor is rotated at  $3^\circ$ , the magnetic field intensity peaks at  $6.976 \times 10^5$  A/m. This high intensity, driven by repulsive forces, aids in rotor movement in the same direction. These findings confirm that optimal magnet positioning can improve rotational efficiency in a magnetic turbine system [18]. However, an anomaly is observed at  $42^\circ$  when the rotor is at  $3^\circ$ , where the magnetic flux density spikes irregularly (4.112 T). This indicates cogging torque issues, which may cause undesired fluctuations in rotor movement. Meanwhile, the  $44^\circ$  configuration exhibits a more stable magnetic flux distribution, suggesting that this angle may be preferable for smoother turbine operation [19].

**Table 5.** Magnetic field intensity (A/m) generated by magnet angle and position data

Angle of attack	Rotor rotation			Information on the position
	$3^\circ$	$6^\circ$	$9^\circ$	
$42^\circ$	$6.976 \times 10^5$	$4.734 \times 10^5$	$6.474 \times 10^5$	Face to face
	$4.650 \times 10^5$	$3.945 \times 10^5$	$4.855 \times 10^5$	Close by
$44^\circ$	$6.280 \times 10^5$	$6.147 \times 10^5$	$6.619 \times 10^5$	Face to face
	$4.710 \times 10^5$	$4.610 \times 10^5$	$4.964 \times 10^5$	Close by

**Table 6.** Magnetic flux density (T) generated by magnet angle and position data

Angle of attack	Rotor rotation			Information on the position
	$3^\circ$	$6^\circ$	$9^\circ$	
$42^\circ$	4.112	$8.248 \times 10^{-1}$	1.161	Face to face
	$6.951 \times 10^{-1}$	$6.873 \times 10^{-1}$	$8.708 \times 10^{-1}$	Close by
$44^\circ$	1.126	1.102	1.07	Face to face
	$8.440 \times 10^{-1}$	$8.269 \times 10^{-1}$	$8.028 \times 10^{-1}$	Close by

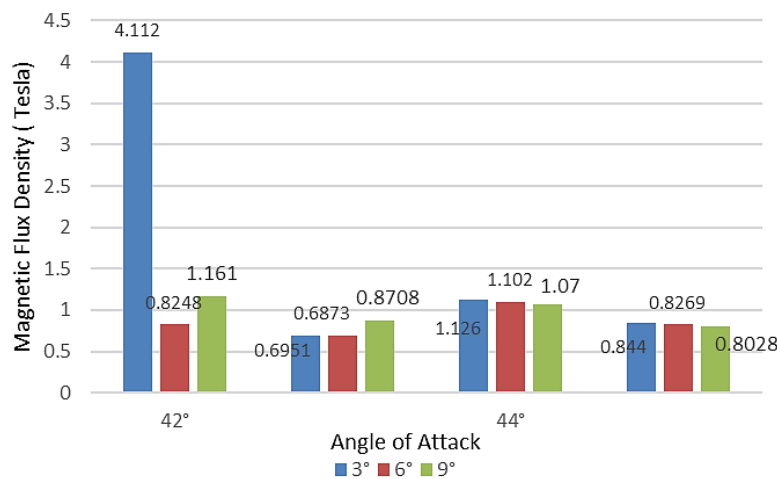


**Fig. 6.** Results of variation of magnet angle and position

#### 4. Discussions

To increase the magnetic force, what can be done is to increase the thickness of the magnet. The thickness of the magnet has a direct effect on the strength of the magnetic field produced [16]. When the thickness of the magnet is not greater than the diameter of the magnet, the distribution of force that occurs when the magnets are close together, there is more magnetic force that attracts each other. Compared with magnets that have a thickness that exceeds the diameter of the magnet, the repulsive force is also greater for magnets that have a thickness that exceeds the diameter of the magnet, with the same distance between the magnets. Magnetic interactions in materials can vary depending on the structure and thickness of the material. Thicker magnets can yield a more consistent force distribution, hence improving the efficacy of repulsion when the magnets are in close proximity. This work proved that magnet thickness substantially affects the intensity of magnetic interaction, with thicker magnets often generating greater repulsion [20].

Attraction forces occur when two magnets are brought close together. This force is distributed when the stator is aligned in a row with a distance of  $12^\circ$  between each magnet. Changes in the angle between the magnets affect the performance of the magnetic motor. So, in designing a magnetic motor, the distance and angle between the magnets to get the best performance should be considered [21]. The other consideration is the cogging force, which is a repulsive force that arises from magnets that are arranged close together. This repulsive force will slow down the rotational momentum of the motor before the motor is finally forced to stop. To overcome the emergence of this cogging force, it can be done by maximizing the design of the large angle planning and the distance between the magnets.

#### IV. Conclusions

The study has succeeded in determining the effect of magnetic field thickness and angle of attack in the rotor and stator design development process on magnetic. The simulation shows that the most efficient magnetic turbine design is a rotor and stator with a magnet size of  $\varnothing 10 \times 20$  mm and an angle of attack of  $44^\circ$ . The thickness of the magnet affects the magnetic force; the thicker the magnet, the stronger the magnetic force, because it stores more magnetic energy. The thinner the magnet size, the weaker the magnetic force, because the magnetization volume is lower. In this simulation, the thickest magnet size that produces the highest magnetic force is  $\varnothing 10 \times 20$  mm. Proving that thickness affects the magnetic force, the thicker the stronger the magnetic force. From the simulation of two magnets facing each other, the magnet size  $\varnothing 10 \times 20$  mm, the angle of attack of  $44^\circ$  gets the highest result of  $2.277 \times 10^{-1}$  Tesla. Meanwhile, the angle of attack between the rotor and stator that is suitable for a magnetic turbine is  $44^\circ$ . These results can be found in Tables 5 and 6, as well as visualization from Figure 6, showing a more stable magnetic flux distribution. So it can avoid cogging torque that can cause unwanted fluctuations in rotor movement. So this angle can produce smoother turbine rotation. In addition, the position of the Neodymium N52 magnet ( $\varnothing 10 \times 20$  mm), which is positioned repelling, can increase the distribution of magnetic force more effectively and can minimize the occurrence of cogging torque. However, it can be underlined that this study is only a simulation without conducting experiments to test the feasibility of the design. Further research is expected to be able to make prototypes and conduct experiments to ensure the feasibility of this design and simulation. In addition, there are still many important things that can be done in the future to contribute to the development of the use of magnetic motors that are useful as renewable energy in the field of electricity, and are expected to be able to improve efficiency related to world electricity needs.

## References

- [1] E. Zondra and H. Yuwendius, "Electrical energy consumption against speed changes of a three-phase induction motor", *Sainetin*, vol. 4, no. 1, pp. 9-18, 2019, doi: 10.31849/sainetin.v4i1.3978.
- [2] M. Yusuf and I. Sara, "Implementation of intelligent systems in the industrial automation workshop building of the Banda Aceh job training center as a solution to saving electrical energy", *National Journal of Electrical Engineering*, vol. 9, no. 2, p. 61, 2020, doi: 10.25077/jnte.v9n2.703.2020.
- [3] F. Ferdianto, "Output power analysis on the performance of synchronous electric motors based on computational", *Telka - Telecommunication Electronics Computing and Control*, vol. 9, no. 2, pp. 107-116, 2023, doi: 10.15575/telka.v9n2.107-116.
- [4] A. Prasetia, "Speed control of brushless direct current (BLDC) motor using a CUK converter based on a fuzzy logic controller", *Electrician Jurnal Rekayasa Dan Teknologi Elektro*, vol. 17, no. 3, pp. 270-276, 2023, doi: 10.23960/elc.v17n3.2478.
- [5] M. Fikri, U. Buana, and D. Santoso, "Design of permanent magnet synchronous generator for 500 watt wind power plant with low wind speed", *Journal of Electrical Engineering and Vocational*, vol. 8, no. 2, p. 200, 2022, doi 10.24036/jtev.v8i2.116750.
- [6] Y. Yılmaz and B. Akgül, "Effects of heat treatment and on magnetic properties of NdFeB based permanent magnet alloys", *European Journal of Science and Technology*, 2022, doi: 10.31590/ejosat.1142054.
- [7] M. Baloyi, "Investigating the magnetic and mechanical properties of ndcefe14b permanent magnets: ab initio study", *Matec Web of Conferences*, vol. 406, p. 02008, 2024, doi: 10.1051/mateconf/202440602008.
- [8] X. Shang, H. Tu, J. Zhang, B. Ni, L. Wang, and M. Wanget, "High coercivity pr2fe14b magnetic nanoparticles by a mechanochemical method", *RSC Advances*, vol. 11, no. 20, pp. 12315-12320, 2021, doi: 10.1039/d1ra01846a.
- [9] M. Baloyi, "The influence of holmium substitution on the magnetic and mechanical properties of nd2fe14b: A first principle study", *Matec Web of Conferences*, vol. 388, p. 07004, 2023, doi: 10.1051/mateconf/202338807004.
- [10] S. Ahmadi, K. Anam, and W. Widjonarko, "Improving energy efficiency in electric vehicles with differential electronics based on ANN (artificial neural network)", *Elkomika: Jurnal Teknik Energi Elektrik, Teknik Telekomunikasi, & Teknik Elektronika*, vol. 8, no. 3, p. 642, 2020, doi: 10.26760/elkomika.v8i3.642.
- [11] M. Zhang, "Permanent magnet synchronous motor demagnetization fault diagnosis based on leakage radial magnetic density", *Journal of Physics Conference Series*, vol. 2708, no. 1, p. 012008, 2024, doi: 10.1088/1742-6596/2708/1/0120.
- [12] M. Deepak, J. Gopalakrishnan, C. Bharatiraja, and L. Mihet-Popa, "Critical aspects of electric motor drive controllers and mitigation of torque ripple—review", *IEEE Access*, vol. 10, pp. 73635-73674, 2022, doi: 10.1109/access.2022.3187515.
- [13] Y. Cao, "Optimal design of asynchronous motor based on finite element simulation", *TCSISR*, vol. 1, pp. 182-192, 2023, doi: 10.62051/kbdh5a71
- [14] Q. Bi and D. Shao, "Loss analysis of high-speed permanent magnet motor for cordless vacuum cleaner", *Journal of Physics Conference Series*, vol. 2488, no. 1, p. 012021, 2023, doi: 10.1088/1742-6596/2488/1/012021.
- [15] F. Hidayanti and E. Wati, "Simulation and testing of cylindrical magnetic turbine design at the center for innovation and certification (cic)", *Helix*, vol. 10, no. 1, p. 13-17, 2020, doi: 10.29042/2020-10-1-13-17.

- [16] M. Mulyadi, "Analysis of mechanical properties, physical properties and magnetism of permanent magnet composite NdFeB with polyvinyl alcohol (PVA) adhesive", *Journal of Disc Mechanical Engineering*, vol. 2, no. 1, p. 29, 2019, doi: 10.32493/jtc.v2i1.2813.
- [17] W. Jannah, M. Syafwan, and R. Lestari, "Analysis of spring-magnet model", *UNAND Mathematics Journal*, vol. 8, no. 2, p. 149, 2019, doi: 10.25077/jmu.8.2.149-156.2019
- [18] H. Putri, Y. Radiyono, and B. Setiawan, "Development of magnetic induction experiment tool on current-carrying coiled wire with hall effect sensor ugn3503", *Journal of Physics Materials and Learning*, vol. 12, no. 1, p. 44, 2022, doi: 10.20961/jmpf.v12i1.61193.
- [19] Z. Dai, J. Li, L. Zou, J. Wang, and R. Luo, "A new high-efficiency double-stator split-pole permanent-magnet vernier machine with flux-focusing topology", *Applied Sciences*, vol. 7, no. 4, p. 356, 2017, doi: 10.3390/app7040356.
- [20] A. Pramurdi, "Design study of radial flux permanent magnet generator in low rotation speed wind power plant", *Cyclotron*, vol. 3, no. 1, 2020, doi: 10.30651/cl.v3i1.4302.
- [21] J.D. Shree, "Implementation of a high power quality BLDC motor drive using bridgeless DC to DC converter with fuzzy logic controller". *Engineering, Technology & Applied Science Research*, 12(5), pp. 9178-9185, 2022, doi: 10.48084/etasr.5213.
- [22] I.R. Sugara, N. Ilminnafik, S. Junus, M.N. Kustanto, and Y. Hermawan, "The combustion characteristics of *Calophyllum inophyllum* fuel in the presence of magnetic field". *Journal of Mechanical Engineering Science and Technology (JMEST)*, 7(1), pp. 28-38, 2023, doi: 10.17977/um016v7i12023p028.